Progressive Collapse of Multi-Storey Buildings due to Failed Floor Impact

A.G. Vlassis[1], B.A. Izzuddin[2], A.Y. Elghazouli[3], D.A. Nethercot[4]

ABSTRACT

This paper proposes a new design-oriented methodology for progressive collapse assessment of floor systems within multi-storey buildings subject to impact from an above failed floor. The conceptual basis of the proposed framework is that the ability of the lower floor for arresting the falling floor depends on the amount of kinetic energy transmitted from the upper floor during impact. Three principal independent stages are employed in the proposed framework, including: (a) determination of the nonlinear static response of the impacted floor system, (b) dynamic assessment using a simplified energy balance approach, and (c) ductility assessment at the maximum level of dynamic deformation attained upon impact. In order to calibrate the proposed method, the part of the kinetic energy of the impacting floor that is transferred to the impacted floor is first theoretically determined for the two extreme impact possibilities, namely *fully rigid* and *fully plastic* impact. Moreover, a series of numerical studies is carried out to further refine the accuracy of this new approach with respect to different impact scenarios, whilst the effects of detailed joint modelling and redundancy are also investigated. The application of the proposed methodology is demonstrated by means of a case study, which considers the impact response of a floor plate within a typical multi-storey steel-framed composite building. Several possibilities regarding the location of the impacted floor plate, the nature of the impact event and the intensity of the gravity loads carried by the falling floor are examined. The application study illustrates the extremely onerous conditions imposed on the impacted floor resulting in an increased vulnerability to progressive collapse for structures of this type. Importantly, the likelihood of shear failure modes in addition to inadequate ductility supply under combined bending/axial actions is identified, thus establishing the need for further research work on the dynamic shear capacity of various connection types subject to extreme events.

Keywords: progressive collapse, floor impact, energy transfer, ductility, steel-framed buildings

---

[1] Former research student, Department of Civil and Environmental Engineering, Imperial College London SW7 2AZ, anastasios.vlassis@imperial.ac.uk

[2] Professor of Computational Structural Mechanics, Department of Civil and Environmental Engineering, Imperial College London SW7 2AZ, b.izzuddin@imperial.ac.uk

[3] Reader in Engineering Structures, Department of Civil and Environmental Engineering, Imperial College London SW7 2AZ, a.elghazouli@imperial.ac.uk

[4] Professor of Civil Engineering, Department of Civil and Environmental Engineering, Imperial College London SW7 2AZ, d.nethercot@imperial.ac.uk

1. Introduction

Sudden column loss is the most common direct design method recommended for progressive collapse mitigation by current design codes and guidelines[1-4]. According to this approach, also referred to as the *alternate load path* method, the potential for progressive collapse may be diminished by designing the structure such that it can bridge across the local failure zone resulting from instantaneous removal of a primary vertical support member. Hence, structural robustness is directly related to the ability of the structure to redistribute the loads and remain stable following this extreme event. The limit state that is considered in association with this design scenario is failure of the floor(s) above the removed column[5-7]. Nonetheless, no matter how unlikely this seems in view of the significant kinetic energy acquired by one or more falling floors following failure, it is still possible under specific circumstances for the lower part of the structure to arrest impact and prevent progressive collapse. The factors that mainly influence this possibility include: i) the number of failed floors above the level under consideration, ii) the reduction in kinetic energy through energy absorption within the failed floors as well as energy loss upon impact, and iii) the ability of the lower structural floor system to sustain the additional load from debris, accounting for the associated dynamic effects.

Detailed modelling of the impact of an upper floor onto the floor below is feasible using current sophisticated nonlinear dynamic analysis software. Yet the computational effort in the case of large and complex structural systems can be excessive, especially if a detailed model of the whole structure is considered. Moreover, such analysis requires structural engineers with considerable expertise in nonlinear structural dynamics. Due to these limitations, detailed impact modelling is not practical for design applications. On the other hand, design approaches based on oversimplified assumptions are not deemed satisfactory either because, even if they err on the conservative side, they may produce unrealistic results. Hence, there is an evident need for simple, yet sufficiently accurate methodologies that can be used to establish whether the strength, ductility supply and energy absorption capacity of the lower impacted floor are adequate to withstand the imposed dynamic loads from the falling floor(s). In this respect, Kaewkulchai and Williamson recently extended the beam element formulation and solution procedure they previously developed for progressive collapse analysis of plane frames[8] to account for the impact of failed members on the structural components below[9]. This work was restricted to plane frames and considered only *plastic impact* scenarios, in

which the impacting and impacted beams are assumed to move at the same velocity after instantaneous impact.

In recognition of both the complexity of the problem in hand and the scarcity of relevant design tools, this paper describes a framework for simplified progressive collapse assessment of floor systems subject to impact from one upper failed floor, though the proposed method can be generalised to deal with the initial failure of more than one floor. Similar to the assessment procedure developed by Izzuddin *et al.* for multi-storey buildings involved in sudden column loss design scenarios[5,6], the proposed approach uses the nonlinear static response of the impacted floor along with an energy balance approach to estimate the maximum dynamic deformation demands without the need for detailed nonlinear dynamic analysis. Focussing on steel-framed buildings with partial-strength joints, the overall ability of the floor system to arrest the impact of the above floor, and thus to prevent progressive collapse, is determined through comparison between the ductility demands induced by the impact and the ductility capacities of the joints within the affected floor.

Since the ability of the lower floor to sustain impact is directly linked to its energy absorption characteristics, the part of the kinetic energy of the impacting floor that is transferred to the impacted floor is theoretically calculated prior to presentation of the method. The calculation is carried out with reference to a simply-supported beam subject to the two extreme impact scenarios, namely a *fully rigid* and a *fully plastic* impact. Building on the outcome of this calculation, the proposed method is calibrated against the results of several numerical studies, in which various ratios of the mass of the impacting to the impacted floor are taken into account, and the effects of detailed joint modelling as well as redundancy are investigated in some detail for both the plastic and rigid impact possibilities.

The application of the proposed approach to steel-framed composite structures with partial-strength joints is demonstrated by means of a case study which considers the impact response of a floor plate within a typical seven-storey steel-framed composite office building. Several possibilities with respect to the location of the impacted floor plate, the nature of the impact event and the intensity of the gravity loads carried by the falling floor are examined. It is concluded that such structures are susceptible to progressive collapse initiated by impact of a failed floor, mainly due to insufficient ductility supply under combined bending and axial deformation modes. Moreover, the development of shear failure modes is identified, thus further increasing the observed vulnerability of the studied floor system. Since these shear

modes of failure are expected to be even more pronounced when the actual dynamic rather than the static response of the impacted floor is considered, the need for further research work focussing on the shear capacity of a variety of connection types subject to extreme events is established. Finally, practical design recommendations that can improve the impact response of floor systems exposed to impact from the floor above are made.

2. Theoretical Calculation of Energy Transfer due to Impact

In general, when a moving body impacts another body at rest, part of the kinetic energy of the impacting body is dissipated on impact, another part is retained by the impacting body, while the rest is imparted to the impacted body. Following impact, the two bodies move with velocities which are different from their initial velocities such that the total momentum of the system remains constant. The two extreme possibilities with regard to an impact problem are a fully plastic and a fully rigid impact[10]. The main feature of a fully plastic impact is that the two bodies attach to each other after the initial collision, and part of the original kinetic energy is lost. The principle of conservation of momentum can be employed to calculate the percentage of the kinetic energy that is transferred to the impacted body. On the other hand, the problem of a fully rigid impact is somewhat more complicated when impact is a result of free fall under the action of gravity, since this scenario involves several bounces of the impacting on the impacted body, leading to energy transfers at various discrete points in time. Importantly, in a fully rigid impact both the principles of conservation of momentum and conservation of energy apply. A theoretical calculation of the energy transfer during the two limiting impact scenarios is presented next with reference to the impact response of a simply-supported beam. The calculation is based on the assumption of a kinematically admissible velocity field for the post-impact motion of the two colliding beams. The shape of this field in each case is determined from the assumed static collapse profile[11], where consideration is given to a basic triangular failure mode.

2.1. Fully Plastic Impact

To determine the energy transfer that takes place in a fully plastic impact, a simply-supported beam of span L is considered under impact by another beam of the same span falling from height h and travelling with initial velocity v_1 just before impact. The uniformly distributed masses of the impacting and impacted beams are m_1 and m_2, respectively. By equating the total potential energy of the upper beam to the kinetic energy acquired at the time it reaches the beam below, it can be easily shown that v_1 is given by:

$$v_1 = \sqrt{2\,g\,h} \tag{1}$$

If a triangular rigid-plastic failure mechanism is assumed for the two combined beams after impact, the single triangular velocity field of Fig. 1 can be considered for both beams. Due to symmetry about the midspan, it is only necessary to consider the portion $0 \le x \le L/2$ of the two beams (Fig. 1).

Conservation of angular momentum of one half of the two beams about the support requires that:

$$\int_0^{L/2} m_1 v_1 \left(\frac{L}{2} - x\right) \mathrm{d}x = \int_0^{L/2} \left(m_1 + m_2\right) v_{mc} \left(1 - \frac{2}{L}x\right)\left(\frac{L}{2} - x\right) \mathrm{d}x \tag{2}$$

in which, as illustrated in Fig. 1, v_{mc} is the joint velocity of the two beams after impact. Assuming that the two beams have the same size and carry equal gravity loads, i.e. $m_1 = m_2 = m$, and solving for v_{mc} we obtain[12]:

$$v_{mc} = \frac{3}{4}\sqrt{2\,g\,h} \tag{3}$$

The relative energy transfer E during impact, expressed as the ratio of the kinetic energy E_2 of the two combined beams immediately after impact to the kinetic energy E_1 of the upper beam immediately before impact, results from:

$$E = \frac{E_2}{E_1} = \frac{\int_0^{L/2} \frac{1}{2}\left(m_1 + m_2\right)\left[v_{mc}\left(1 - \frac{2}{L}x\right)\right]^2 \mathrm{d}x}{\int_0^{L/2} \frac{1}{2} m_1 v_1^2 \,\mathrm{d}x} \tag{4}$$

Using again $m_1 = m_2 = m$ and substituting Eq. (3) into Eq. (4), the resulting relative energy transfer is E = 37.5%. Accordingly, the dissipated energy in a fully plastic impact of two identical beams is equal to 62.5% of the initial kinetic energy of the impacting beam, provided the assumed triangular velocity field gives a good approximation of the actual response.

2.2. Fully Rigid Impact

The main difference between a fully plastic and a fully rigid impact is that there is no energy dissipation in the latter case. Moreover, the two colliding beams do not remain in contact after impact but deform individually, hence two independent velocity fields, one for each beam, need to be assumed. The same assumptions as before regarding the properties of the two beams are also made in the fully rigid impact case. It is noted that only the energy transfer associated with the first rebound of the falling beam on the impacted beam is obtained herein. It is anticipated that the actual part of the initial kinetic energy transferred to the lower beam at the end of the impact event will be relatively higher due to the subsequent bounces that will occur.

Considering the rebound velocities of the upper beam following impact, the velocity at the midspan will not generally be equal to the velocity at the two supports. Therefore, assuming that the impacted beam will deform in a triangular mode, the transverse velocity fields illustrated in Fig. 2 may be considered for the two beams. It is noted that, similar to the previous case, only the portion $0 \le x \le L/2$ of the two beams is considered due to symmetry.

Applying again conservation of angular momentum about the support to the right half of the two colliding beams we obtain:

$$\begin{aligned} &\int_0^{L/2} m_1 v_1 \left(\frac{L}{2}-x\right) \mathrm{d}x = \int_0^{L/2} m_2 v_m \left(1-\frac{2}{L}x\right)\left(\frac{L}{2}-x\right) \mathrm{d}x + \ldots \\ &+ \int_0^{L/2} m_1 \left(-v_{rm}-\frac{2v_{rs}-2v_{rm}}{L}x\right)\left(\frac{L}{2}-x\right) \mathrm{d}x \end{aligned} \tag{5}$$

in which, as shown in Fig. 2, v_{rm} and v_{rs} are the rebound velocities of the upper beam at the midspan and the supports, respectively, v_m is the velocity of the lower beam at the midspan, and v_1 is the uniform velocity of the falling beam immediately before impact given by Eq. (1). To ensure that the exchange of momentum is compressive along the full beam length, v_m should be always positive. Furthermore, the physical constraints $v_{rm} \ge -v_m$ and $v_{rs} \ge 0$ should be observed[13].

Taking two identical beams into account and performing the integrations, Eq. (5) can be rewritten in the following form:

$$3\sqrt{2gh} = 2v_m - 2v_{rm} - v_{rs} \tag{6}$$

In addition to conservation of momentum, the kinetic energy immediately before and after impact should also be conserved in a fully rigid impact:

$$\int_0^{L/2} \frac{1}{2} m_1 v_1^2 \, \mathrm{d}x = \int_0^{L/2} \frac{1}{2} m_2 \left[v_m \left(1 - \frac{2}{L} x \right) \right]^2 \mathrm{d}x + \int_0^{L/2} \frac{1}{2} m_1 \left(-v_{rm} - \frac{2 v_{rs} - 2 v_{rm}}{L} x \right)^2 \mathrm{d}x \tag{7}$$

which gives for the case $m_1 = m_2 = m$:

$$6 g h = v_m^2 + v_{rm}^2 + v_{rs}^2 - v_{rm} v_{rs} \tag{8}$$

Based on Eqs. (6) and (8), it is clear that the post-impact velocity fields are not uniquely defined using conservation of energy and momentum in the fully rigid impact case. Yet, solving the system of Eqs. (6) and (8) we can obtain the velocities v_m and v_{rm} at the midspan of the two beams as functions of the initial storey height h and the rebound velocity v_{rs} at the two ends of the upper beam:

$$v_{m1,2} = \frac{3}{4} \sqrt{2 g h} \pm \frac{\sqrt{30 g h - 6 v_{rs}^2}}{4} \tag{9}$$

$$v_{rm1,2} = -\frac{v_{rs}}{2} - \frac{3}{4} \sqrt{2 g h} \pm \frac{\sqrt{30 g h - 6 v_{rs}^2}}{4} \tag{10}$$

Considering a typical storey height of 4m and using the velocities of Eqs. (9) and (10), we can determine the part of kinetic energy that is imparted to the impacted beam in a fully rigid impact for several values of the rebound velocity v_{rs} (Table 1). It should be noted that the limit value of v_{rs} is governed by the constraint $v_{rm} \geq - v_m$, which for h = 4m yields v_{rs} = 12.97m/s. As shown in Table 1, the relative energy transfer E associated with a fully rigid impact scenario can greatly vary between 41% and 98%, depending on v_{rs}, although it is generally greater than 70%.

3. Proposed Progressive Collapse Assessment Methodology

When a floor fails and falls onto the floor below, the impulse transmitted to the lower system results in the development of considerable ductility demands that, for the very common structural class of steel-framed buildings with partial-strength joints, mainly affect the support joint regions within the impacted floor[13]. The magnitude of these demands, which are

generally significantly higher than those associated with a sudden column loss scenario[7,12,13], is attributed to the significant amount of kinetic energy acquired by the upper floor immediately prior to impact. Depending on the particular characteristics of the impact event, the theoretical calculation discussed in the previous section has shown that the percentage of the imparted energy can vary from approximately 40% to nearly 100% of the initial energy for fully plastic and fully rigid impact scenarios, respectively. As a consequence, the vertical impact of the upper floor onto the lower floor applies massive vertical dynamic loads on the underlying floor system, greatly challenging its dynamic load carrying and deformation capacities. The situation can become even more untenable if multiple floors rather than a single floor fail and crash on the structure below, or if the falling floor disintegrates completely prior to impact retaining no residual strength and/or spanning capability.

A simplified assessment framework is described in this section that can be used in association with floor impact scenarios to evaluate the potential of the lower impacted floor for arresting the falling floor and, thus, preventing progressive collapse. Due to the similarities of the two problems, the proposed methodology is largely based on the corresponding framework developed by Izzuddin *et al.*[5,6] for assessing the consequences of sudden column removal. In this respect, the ability of a floor system subject to failure and subsequent impact of the floor above to withstand the imposed loads and prevent progressive collapse is assessed by employing three independent stages, namely: i) determination of the nonlinear static response, ii) simplified dynamic assessment, and iii) ductility assessment, which are discussed in detail hereafter.

Knowledge of the nonlinear static response of the impacted floor constitutes the main platform for assessment. Depending on the required level of sophistication and the availability of analytical tools, the static floor response can be established using either detailed or simplified modelling techniques, the relative benefits of which are discussed elsewhere [5-7,13]. Upon establishment of the nonlinear static response, the axes of the static response P-u_s curve are shifted to account for the initial deformations of the lower floor due to the original gravity loads before impact (Fig. 3). Thus, the resultant P′-u'_s curve is used in the following dynamic assessment stage of the proposed procedure to determine the ductility demands induced to the floor components as a result of the collision of the upper floor.

It is further assumed that the dynamic effects associated with floor impact can be reasonably reproduced by considering the gravity load carried by the upper floor to be applied

instantaneously on the lower floor[13]. Hence, an energy equilibrium approach is employed to estimate the maximum dynamic deformation demands imposed on the lower impacted floor, thus avoiding the performance of computationally demanding nonlinear dynamic analysis. According to this approach, the point of stationary equilibrium following impact is reached when the difference between the strain energy absorbed by the impacted floor system, as it deforms downwards, and the work done by the upper floor gravity load, effectively applied as a step load, becomes equal to the part of the original kinetic energy that is imparted to the lower floor in line with the assumed impact scenario. It is noted that this approach presupposes that a single mode of deformation will dominate the floor response following impact. In this case, the actual load distribution on the impacted floor components does not affect the incremental energy absorption capacity of the floor, especially for the magnitude of deformations that are expected to develop due to impact[5,6,13].

Application of the energy equilibrium approach is illustrated in Figs. 3a and 3b for two distinct impact scenarios related to two different levels of gravity loading sustained by the upper floor prior to failure. It is noted that the original static response P-u_s curve, which includes the effect of the gravity loads carried by the lower floor system before impact, is also shown. With reference to the shifted static response P′-u'_s curve, the first level of impact loading is $P' = 0.50\ P_o$ and corresponds to the case that the falling floor carries one half of the gravity loads of the lower floor, while in the second case $P' = 1.00\ P_o$ (i.e. the two floors are assumed to originally carry equal gravity loads). The maximum dynamic displacements $u'_{d,1}$ and $u'_{d,2}$ in each case are attained when the difference between the work performed by the instantaneously applied gravity loading (area under the step load curve) and the energy dissipated internally (area under the shifted nonlinear static load-deflection curve) becomes equal to the kinetic energy transferred according to the specific level of impact loading and assumed plastic/rigid impact scenario (area with vertical hatching). In the general case that the level of the suddenly applied gravity loading that is imparted from the impacting floor is $P'_n = \lambda_n P_o$, the external work W'_n done by this loading up to a dynamic displacement $u'_{d,n}$ can be obtained from:

$$W'_n = \alpha \lambda_n P_o u'_{d,n} \tag{11}$$

Furthermore, the strain energy U'_n absorbed by the impacted floor following impact is given by:

$$U'_n = \int_0^{u'_{d,n}} \alpha P' du'_s \tag{12}$$

It is noted that α in Eqs. (11) and (12) is a non-dimensional weighting factor which depends on the assumed gravity load distribution on the floor components[5,6,13].

Finally, the amount of energy transfer $E_{T,n,i}$ during impact corresponding to the impact loading P'_n and impact scenario i can be obtained from:

$$E_{T,n,i} = \gamma_i \lambda_n P_o h \tag{13}$$

where γ_i is a non-dimensional reduction factor related to the percentage of the initial kinetic energy of the impacting floor that is imparted to the impacted floor in line with the anticipated impact characteristics, and *h* is the original storey height.

Hence, setting the difference $U'_n - W'_n$ equal to $E_{T,n,i}$ and solving for $P'_n = \lambda_n P_o$ we obtain:

$$P'_n = \lambda_n P_o = \frac{\alpha \int_0^{u'_{d,n}} P' du'_s}{\alpha u'_{d,n} + \gamma_i h} \tag{14}$$

Providing the main features of the impact event and the resulting energy transfer from the upper to the lower floor can be predicted with reasonable accuracy, Eq. (14) may be used to determine the level of the suddenly applied gravity loading P'_n that results in a particular maximum dynamic displacement $u'_{d,n}$ of the impacted floor system. Besides, similar to the case of structural systems subject to sudden column loss scenarios[5,6,13], the overall maximum nonlinear impact response of the floor system under consideration may be expressed in terms of a P'-u'_d curve, which, as illustrated in Fig. 3c, can be created by plotting the suddenly applied gravity loading P'_n at each load level n versus the corresponding maximum dynamic displacement $u'_{d,n}$. To distinguish this response from the pseudo-static response defined with reference to instantaneous column removal[5,6,13], the term *modified pseudo-static response* is used in the current context, since it also accounts for the additional energy introduced into the system due to impact. Thus, based on the magnitude of the gravity loads sustained by the upper floor before failure, taken as a proportion of the initial lower floor loads P_o, the maximum dynamic deformation of the impacted floor system can be obtained directly from the modified pseudo-static response.

In order to facilitate the procedure, a simple algorithm can be devised to obtain the modified pseudo-static response P'-u'_d curve when the shifted nonlinear static response P'-u'_s curve of the floor system as well as the energy transfer factor γ_i associated with the assumed impact scenario are known. Also, the maximum dynamic displacement resulting from a specific instantaneously applied impact loading λP_o can be established. A notation consistent with Fig. 3 is used with $P'_{m\backslash n}$ representing the instantaneously applied gravity load $\lambda_{m\backslash n} P_o$, $P'_{d,m\backslash n}$ denoting the amplified static load $\lambda_{d,m\backslash n} P_o$, and m and n indicating the start and end of the current increment, respectively. Hence, the required steps for obtaining the modified pseudo-static response P'-u'_d curve are as follows:

1. Initialise: $P'_{d,m} = P'_m = 0$, $u'_{d,m} = 0$, $A'_m = 0$;
   choose a small displacement increment $\Delta u'_d$
2. Set: $u'_{d,n} = u'_{d,m} + \Delta u'_d$
3. Determine $P'_{d,n}$ corresponding to $u'_{d,n}$ from shifted static response P'-u'_s curve;
   obtain current area under the P'-u'_s curve: $A'_n = A'_m + (P'_{d,m} + P'_{d,n})\, \Delta u'_d/2$
4. Determine the current modified pseudo-static load: $P'_n = \alpha\, A'_n/(\alpha\, u'_{d,n} + \gamma_i\, h)$;
   establish new point $(P'_n, u'_{d,n})$ on modified pseudo-static response P'-u'_d curve
5. If $P'_m < \lambda P_o \leq P'_n$, obtain and output dynamic displacement u'_d corresponding to λP_o:
   $u'_d = u'_{d,m} + (u'_{d,n} - u'_{d,m})\, (\lambda P_o - P'_m)/(P'_n - P'_m)$
6. If more points are required for modified pseudo-static response curve:
   update: $P'_{d,m} = P'_{d,n}$, $P'_m = P'_n$, $u'_{d,m} = u'_{d,n}$, $A'_m = A'_n$;

   repeat from step 2.

According to the last stage of the proposed assessment methodology, the dynamic deformation demand established from the modified pseudo-static response for the assumed impact scenario can be translated into ductility demands on the various floor components. These can subsequently be compared to the available ductility supply of the components to assess the overall ability of the lower floor to withstand impact and prevent progressive collapse. With particular reference to steel-framed buildings with partial-strength joints, the floor limit state is associated with failure of a single joint, which is assumed to occur when the ductility demand exceeds the ductility capacity in one or more of the joint components[6,7]. However, this approach may be unrealistically onerous for floor systems in which there is sufficient residual redundancy and ductility following failure of a relatively non-ductile joint detail. In such cases, the failed joint along with the connected floor component should be

disregarded and the susceptibility of the remaining floor system to progressive collapse due to impact of the floor above should be re-evaluated[6].

As a general remark on its applicability, it is evident that the proposed simplified assessment framework presents several advantages, since it explicitly accounts for the nonlinearity of floor response upon impact, while it also facilitates the use of both simplified and detailed modelling techniques. Furthermore, it takes the dynamic nature of the impact event into account, without resorting to computationally demanding detailed nonlinear dynamic analysis, through an energy balance approach.

4. Calibration of the Proposed Methodology

The accuracy of the assessment methodology presented in the previous section is directly dependent on the accurate prediction of the amount of energy transfer that takes place during impact. In this respect, a series of numerical studies is carried out hereafter in order to calibrate the proposed method with respect to different impact scenarios. To investigate the relationship between the gravity loads carried by the two floors and the amount of energy imparted to the lower floor, various ratios of the mass of the impacting to the impacted floor are taken into account, whilst the effects of detailed joint modelling and redundancy are also examined in some detail.

4.1. Plastic Impact Case

Based on the theoretical calculation of Section 2, the percentage of energy transfer during a fully plastic impact of two identical floor beams is approximately 40% of the kinetic energy acquired by the falling beam immediately before impact. To verify this value, the impact response of a two-dimensional finite element floor beam model with partial-strength support joints is considered. The developed model, which accounts for geometric and material nonlinearity, consists of an I-section steel beam (flanges: $210.0\times17.2\text{mm}^2$, web: $515.6\times11.1\text{mm}^2$) with Young's modulus $E_s = 210\times10^3\text{N/mm}^2$, yield strength $\sigma_y = 235\text{N/mm}^2$, and 1% strain-hardening factor. Regarding joint modelling, a simplified approach is adopted with the support joints represented by spring elements that exhibit uncoupled elastic-perfectly plastic axial and rotational responses. The flexural stiffness and strength of the support joints are taken as $3E_sI_b/L$ and $30\%M_p$, where I_b and M_p are the second moment of area and the plastic moment capacity of the beam cross-section, respectively, and L is the span of the floor beam. It is noted that the axial restraint at the beam ends from the neighbouring structural members is ignored in this specific calibration study[13].

In order to investigate the effect of the relative intensity of the gravity loads carried by the two floors on the impact response, two further mass ratios equal to $m_1/m_2 = 0.5$ and $m_1/m_2 = 2.0$ in addition to $m_1/m_2 = 1.0$ are taken into account, thus corresponding to the cases where the loads of the upper beam are half and double the loads of the lower beam, respectively. Finally, two beam spans equal to L = 8m and L = 20m and an initial storey height h = 4m are considered.

To establish the maximum dynamic response, the model is first considered with detailed nonlinear dynamic analysis using the nonlinear structural analysis program ADAPTIC[14], where plastic impact is represented by the application of a uniform initial velocity on the beam calculated from conservation of linear momentum for a series of infinitesimal masses. Hence, the common post-impact velocity v_c of the two beams in terms of their respective uniformly distributed masses m_1 and m_2 and the velocity v_1 (Eq. (1)) of the falling beam immediately before impact is given by:

$$v_c = \frac{m_1}{m_1 + m_2} v_1 \tag{15}$$

which for $m_1/m_2 = 0.5$, 1.0 and 2.0 yields 2.95m/s, 4.43m/s and 5.91m/s, respectively. Table 2 summarizes the maximum midspan deflection $u'_{d,max}$ attained by the two combined beams following impact for the various modelling assumptions with regard to the mass ratio and beam span. As expected, $u'_{d,max}$ increases with increasing gravity loads of the falling beam. In this respect, when the upper beam carries double the loads of the lower beam, the resulting maximum dynamic displacements corresponding to both spans are unrealistically large, and thus unlikely to be sustained.

In line with the proposed assessment methodology, static analysis of the beam model is also performed under proportionally varied uniformly distributed load (UDL) to obtain its nonlinear static response P-u_s curve, which is subsequently modified to a shifted P′-u'_s curve by excluding the effect of the original gravity loads. Hence, the strain energy U' dissipated internally as the impacted beam deforms towards its maximum deformation can be determined from the area under the P′-u'_s curve up to the corresponding displacement $u'_{d,max}$ obtained from dynamic analysis. Moreover, the work W' done by the instantly applied impact loading up to the same displacement can also be calculated and subtracted from U' to estimate the amount of energy transfer E_T during impact. Since the beam is assumed to sustain a UDL

and deform according to a triangular mode, the weighting factor α used in Eqs. (11) and (12) for calculating W' and U' is taken as 0.5[5,6,13]. The resulting U', W' and E_T values are given in Table 3, where the energy transfer in each case is also expressed as a percentage of the kinetic energy E_K of the falling beam immediately before impact. It can be seen that, when an 8m-long beam is considered, the amount E_T of the energy imparted to the lower beam varies from 25.5% to 48.1% of the original kinetic energy E_K as the mass ratio increases from 0.5 to 2.0. The corresponding range of E_T/E_K for L = 20m is similar to that for L = 8m, varying from 26.1% to 51.4%.

The accuracy of the results presented above is further scrutinized by using a more sophisticated floor beam model which allows for composite action as well as interaction between bending and axial actions within the support joints. The developed finite element model, which is similar to that shown in Fig. 3 of [7], has a span of 10m. The steel beam employs an I-shape UC356×368×153 section with material properties $E_s = 210\times10^3$N/mm^2, σ_y = 355N/mm^2, and 1% strain-hardening factor. The concrete 'flange' is cast on metal decking with a dovetail profile and has an effective width of 3000mm and a total depth of 70mm that only accounts for the concrete above the slab ribs, since the ribs run perpendicular to the beam. The material properties are $E_{lcm} = 27.3\times10^3$N/mm^2 and f_{lc} = 30N/mm^2 for the concrete, and $E_s = 200\times10^3$N/mm^2, σ_{sy} = 460N/mm^2 and 1% strain-hardening factor for the rebars. A 2% reinforcement ratio uniformly distributed along the beam and full shear connection are also assumed. With regard to the support joints, a mechanical model similar to that shown in Fig. 6b of [7], which represents a major axis partial-depth flexible end-plate beam-to-column joint, is employed at the two beam supports[7,13,15]. Finally, no axial restraint from the adjacent structural members is taken into account.

The original UDL carried by the lower floor beam is taken as 16.3kN/m. This value corresponds to a level of service loads at the time of floor impact taken as DL + 0.25 IL[1], where DL and IL are the dead and imposed loads acting on the floor plate, and unfactored dead and imposed floor loads equal to 4.2kN/m^2 and 5.0kN/m^2, respectively[13]. Moreover, similar to the previous simplified model, three ratios of the mass of the impacting to the impacted beam equal to 0.5, 1.0 and 2.0 are accounted for. Again, dynamic analysis is first performed to determine the maximum dynamic deformation $u'_{d,max}$ of the two combined beams following plastic impact of the upper beam. The resulting midspan deflections range from 142.1mm for m_1/m_2 = 0.5 to 947.7mm for m_1/m_2 = 2.0. The nonlinear static response of the composite beam is subsequently established and shifted accordingly, and thus the internal

strain energy U' and the external work W' corresponding to the maximum dynamic displacement in each case can be calculated. As demonstrated in Table 4, the amount of energy transfer E_T associated with the three assumed mass ratios is in excellent agreement with the results obtained from the simplified beam model (Table 3), varying from 25.7% to 50.0% of the kinetic energy E_K acquired by the falling beam immediately before impact. It is noted that a weighting factor $\alpha = 0.5$ is again utilized for the energy calculations in line with the assumed UDL distribution on the beam and a triangular deformation mode[5,6,13], while E_K is determined based on an initial storey height of 4m. In view of the results of the simplified and the detailed beam models, it can be concluded that the energy transfer between two floor beams that collide in a plastic manner is relatively unaffected by the presence of composite action as well as by the level of sophistication adopted in modelling the joint behaviour.

To investigate the possible effects of redundancy on the impact response of two floor systems involved in a plastic impact scenario, a grillage floor system is now considered. As shown in the plan view of Fig. 4, the member sizes of the floor components are UB406×140×39 and UB305×102×25 for the primary and the secondary beams, respectively, while the material properties are $E_s = 210\times10^3$N/mm^2, $\sigma_y = 355$N/mm^2, and 1% strain-hardening factor. Furthermore, simple connection details with uncoupled axial and moment actions are assumed for the support joints of all members[13].

The same three cases as in the previous two-dimensional beam models are also taken into account for the grillage system with respect to the relative magnitude of the gravity loads sustained by the two impacting floors. The intensity of the UDL on the secondary beams of the lower grillage prior to impact is assumed equal to 6.0kN/m. It is noted that this relatively low value has been deliberately selected to facilitate the performance of dynamic analysis, since even under these very light loads the impacted system exhibits very large deformations. To simulate plastic impact, all secondary beams are subjected to a uniform initial velocity field determined from conservation of linear momentum as explained above. The maximum deflections at the midspan of the primary beam obtained from dynamic analysis are 444.7mm, 764.4mm and 1138.6mm for $m_1/m_2 = 0.5$, 1.0 and 2.0, respectively. These displacements are used in conjunction with the shifted static response P'-u'_s curve, which is established when the secondary beams of the grillage are subjected to proportionally varied UDL, to estimate the strain energy U' dissipated internally and the work W' done by the impact loading. Thus, the amount of energy E_T imparted to the lower floor grillage due to plastic impact can be determined and expressed as a percentage of the original kinetic energy E_K of the falling

floor. Since all secondary beams are assumed to sustain a UDL of equal intensity, the weighting factor α for the considered grillage system under the obtained deformation mode can be calculated as follows to satisfy work equivalence[7,13]:

$$\alpha = \frac{0.5 + 2 \times 0.5 \times 0.814 + 2 \times 0.5 \times 0.447}{5} = 0.352 \tag{16}$$

in which 0.814 and 0.447 are respectively the average ratios of the deflections at the third- and sixth-spans of the primary beam to its midspan deflection (Fig. 5).

Table 5 summarizes the calculated values of U', W', E_T and E_K for the three mass ratios considered. It is observed that the estimated percentage of energy transfer is generally lower for the grillage floor system in comparison with the individual beams examined before. Moreover, the reduction in E_T increases with increasing intensity of impact loads. As shown in Fig. 5, due to the effects of redundancy, the deformation mode associated with the grillage system exhibits relatively localized deformations along the secondary beams on either side of the primary beam, which is largely responsible for the reduction in the energy transfer[13].

In summary, as illustrated in Fig. 6 which depicts the variation of E_T/E_K with the mass ratio m_1/m_2 of the two floors, when the beneficial effects of redundancy are ignored, the amount of energy transfer E_T during plastic impact of an upper floor onto the floor below generally varies from approximately 25% to 50% of the original kinetic energy E_K of the falling floor, with the higher percentages resulting from heavier impacting floors. It is noteworthy that these results are in excellent agreement with the relative energy transfer E obtained from Eq. (4) based on a triangular mode of deformation, which is also plotted in Fig. 6. On the other hand, the deformation mode associated with a redundant grillage floor system typically results in a smaller percentage of energy transfer compared to the individual beams, especially for mass ratios greater than one. In this case, rather than a triangular deformation mode, the components of the impacted floor exhibit more localized deformations that reduce the imparted energy.

4.2. Rigid Impact Case

The main feature of rigid impact, as indicated by the theoretical calculation of Section 2, is that the energy transfer is typically higher than that corresponding to plastic impact, and under certain circumstances it can reach nearly 100% of the original kinetic energy of the falling floor. Advanced numerical studies carried out by Vlassis[13], in which contact elements were

employed to simulate rigid impact between two floor beams, established that the most conservative deformations result when the upper floor falls as debris and impact occurs simultaneously along the entire length of the lower beam. It is worth noting that the assessment methodology proposed in Section 3 of this paper assumes that there is a transfer of kinetic energy during impact and the additional loads continue to be exerted as dynamic loads[13]. Unlike the plastic impact case, this assumption is not strictly true for rigid impact; however, the approach is calibrated to estimate the energy transfer on this basis. Therefore, to obtain an upper bound estimation of the amount of energy imparted to the impacted floor, the response of a two-dimensional floor beam model subject to rigid impact from an above failed floor, which disintegrates completely and falls as debris (Fig. 7), is studied in some detail. The model represents an axially unrestrained steel beam with simplified partial-strength joints and material properties E_s = 210×10^{3}N/mm^2, σ_y = 235N/mm^2, and 1% strain-hardening[13]. The upper floor debris is simulated by a series of lumped masses which fall simultaneously onto the lower floor beam, with contact elements utilized to model rigid impact[16]. Similar to the plastic impact case, three mass ratios equal to m_1/m_2 = 0.5, 1.0 and 2.0 are considered so as to investigate whether the magnitude of the gravity loads carried by the upper floor beam has a significant effect on the energy transfer.

Table 6 summarizes the maximum deflections $u'_{d,max}$ at the midspan of the impacted steel beam obtained from dynamic analysis for the three mass ratios and the two beam spans of 8m and 20m accounted for. It is observed that rigid impact typically leads to higher displacements than those associated with plastic impact (Table 2). Upon establishment of the maximum dynamic response of the beam, its nonlinear static response under proportionally varied UDL is also determined and shifted to exclude the effect of the original gravity loads. Hence, based on the resultant P′-u'_s curve, the internal strain energy U' and the external work W' up to the corresponding $u'_{d,max}$ can be obtained and subtracted to estimate the amount of energy E_T imparted to the lower beam in each case. Again, the weighting factor α for determining U' and W' is taken as 0.5, which is consistent with a UDL distribution and a triangular deformation mode [5,6,13]. As shown in Table 7, unlike the plastic impact case, the ratio of the energy transfer E_T to the initial kinetic energy E_K for rigid impact is rather insensitive to the relative intensity of the gravity loads sustained by the two floors before impact, ranging between 51.6% and 53.8% for L = 8m and between 50.8% and 57.7% for L = 20m.

To verify this observation further, a detailed composite beam model with major axis partial-depth flexible end-plate support joints is also considered. Apart from assuming a smaller

effective width of 1500m instead of 3000m for the concrete 'flange' and a bilinear rather than a rigid-plastic shear response for the support joints to overcome numerical instabilities associated with dynamic analysis[13], the model is identical to that discussed in the previous section with reference to plastic impact. Rigid impact is again simulated using contact elements, while complete disintegration of the upper floor before it reaches the floor below and simultaneous impact are assumed. Finally, the same three mass ratios of the two impacting beams as in the simplified steel beam model are considered.

The maximum dynamic midspan deflections $u'_{d,max}$ attained by the lower beam after impact are equal to 192.3mm, 319.6mm and 659.0mm for m_1/m_2 = 0.5, 1.0 and 2.0, respectively. Subsequently, the composite beam model is also considered with static analysis and, after shifting the axes of the nonlinear static response P-u_s curve, the strain energy U' dissipated internally and the work W' done by the impact loading are determined in each case to estimate the amount of energy transfer E_T during impact. It is noted that, similar to the previous case, the weighting factor α in Eqs. (11) and (12) is taken as 0.5. The resulting values of U', W' and E_T along with the corresponding kinetic energy E_K of the falling beam are given in Table 8. It can be seen that the percentage of the energy imparted to the impacted beam is relatively higher compared to the previous simplified steel beam model, varying from 62.4% for m_1/m_2 = 1.0 to 71.3% for m_1/m_2 = 0.5. Although other factors may also be responsible, a plausible explanation for this increase in the E_T/E_K ratio is the increased flexibility in shear exhibited by the support joints of the composite beam model as opposed to the simplified model, in which full shear restraint is provided at the beam ends. Nevertheless, the amount of energy transfer does not appear to vary in proportion to the mass ratio of the two beams, thus confirming the conclusion drawn before that rigid impact is not particularly affected by the magnitude of the original gravity loads sustained by the upper floor.

5. Application Study

The application of the proposed method to steel-framed composite structures with partial-strength joints is demonstrated in this section by means of a case study which investigates the impact response of a floor plate within a typical seven-storey building designed for office use.

5.1. Overview of Floor Impact Case Study

The considered steel-framed composite building, described in detail elsewhere[7,13], consists of seven identical floors in terms of structure and loading and has a storey height of 3.5m. Each floor is designed to sustain uniformly distributed dead and imposed loads with unfactored

values of 4.2kN/m^2 and 5.0kN/m^2, respectively. With regard to the joints, simple connection details that satisfy code prescribed tying force requirements[17] are generally employed with partial depth flexible end-plates utilized for the beam-to-column joints and fin plates for the beam-to-beam joints[18].

Figure 8 shows the geometry of the single floor plate exposed to impact from an upper floor. To achieve a realistic assessment that accounts for three-dimensional effects, which as pointed out above can potentially play a significant role in determining the fraction of kinetic energy transferred from the upper to the lower floor, a grillage-type approximation is adopted for establishing the nonlinear static response of the impacted plate. Although detailed slab modelling that may provide a more realistic representation of planar membrane effects is not explicitly considered, the developed grillage system provides an approximation of membrane effects via catenary action in the beams, while it is also capable of simulating composite action between the steel beams and the concrete slab on metal decking. More importantly, the adopted approach accommodates detailed mechanical joint models[13,15] that can effectively replicate joint behaviour with respect to both the ductility demand on the individual joint components as well as the interaction between bending moment and axial force, the latter being important when the boundaries of the impacted floor system are subject to considerable axial restraint from the surrounding structure[5,6,13]. Finally, to account for two different scenarios with respect to the location of the impacted floor plate, the transverse primary beam (Fig. 8) is assumed to be either axially unrestrained or partially restrained corresponding to a peripheral or an internal floor plate, respectively. It should also be noted that the effect of non-structural elements is not included in the current application study, even though it can be readily accommodated by the proposed assessment framework.

As noted above, the adopted limit state for the grillage floor system is associated with failure of a single support joint in one of the grillage components, which occurs when the ductility capacity of the critical component within this particular joint, determined from explicit joint failure criteria based on relevant experimental and numerical data, is exceeded[13,19-22]. In this respect, in addition to component failure mechanisms which arise under combined bending and axial deformations, it is important that other, perhaps less well understood, modes of failure be also taken into account. Such modes include joint shear failure or local buckling in the compressed regions of the steel members due to local exceedance of their crushing resistance. As explained in the following section, the development of such failure modes may considerably compromise the ductility supply of the joints, and thus they should be carefully

investigated, particularly since it is likely that at least the shear mode may be amplified by the dynamic nature of the actual impact event beyond what is allowed for in the proposed pseudo-static approach.

5.2. Impact Response of Grillage Floor System

To obtain the static response of the grillage system, which constitutes the first stage of the proposed assessment methodology, the gravity load is apportioned to the longitudinal secondary beams assuming a UDL distribution pattern as shown in Fig. 9b. Due to the floor plate geometry, the tributary areas of all secondary beams are 3m-wide (Fig. 8). In this respect, the beams are subjected to proportionally varied UDL of equal intensity, and static analysis is performed using ADAPTIC[14]. Regarding the original gravity loads carried by the floor plate before impact, if a DL + 0.25 IL service load combination is used[1], the apportioned total UDL on each double-span secondary beam with a total length of 12m is $P_{o,SB}$ = 195kN, thus resulting in a total floor gravity load P_o = 585kN. Again, it is important to note that, even though a realistic load distribution on the floor components is beneficial, the accuracy of the proposed method depends mainly on the dominance of a single mode of deformation rather than the actual load pattern.

5.2.1. Nonlinear Static Response

Figures 10a and 10b present the nonlinear static response of the grillage system representing a peripheral and an internal floor plates, respectively. It is noted that the total load P applied to the system is plotted versus the deflection u_s in the middle of the plate, which because of the floor geometry coincides with the midspan deflection of the intermediate longitudinal double-span secondary beam (Fig. 9b). It can be observed that the static response is relatively insensitive to the provision of axial restraint at the supports of the transverse primary beam, and hence to the location of the considered floor plate. Moreover, in both cases, the floor limit state is associated with shear failure, which is assumed to occur when the shear capacity of the support joints of the secondary beams is exceeded. As expected, the support joints of the intermediate secondary beam fail first, thus determining the overall system failure, followed by the joints at the supports of the remaining longitudinal beams, which due to symmetry fail concurrently. As a result of shear failure, the deformation capacities of the peripheral and internal floor plates are respectively limited to approximately 228mm and 225mm. In addition, their static load carrying capacities are both equal to around 2550kN, i.e. roughly 4.4 times the service gravity load assumed to be sustained by the grillage floor system before impact.

It is worth noting that, as long as the shear mode of failure is guaranteed to be ductile for the two floor systems, their nonlinear static response can be substantially enhanced. With reference to the peripheral floor plate case, the subsequent failure would then be governed by reinforcement rupture at the support joints of the intermediate secondary beam. In view of this ductile mode of failure, the floor deformation capacity increases to 474mm, while the static load carrying capacity also improves to a lesser degree reaching 3105kN.

The development of shear failure is primarily attributed to the presence of alternative load paths associated with the transverse primary beam. Due to the upward resistance of the transverse beam, the floor gravity load imposed on the longitudinal secondary beams is effectively distributed towards their outer supports leading to an increased shear force demand at the support joints. This factor combined with the comparatively low shear capacity of the fin plate beam-to-beam joints (160kN) employed at the beam supports is deemed responsible for the premature shear failure[13].

With respect to the deformed shape of the grillage system, as illustrated in Fig. 11 for the peripheral floor plate, the nonlinear static response is indeed dominated by a single mode of deformation. Moreover, the ratio of the deflection at the midspan of the two outermost double-span secondary beams to the midspan deflection of the middle beam is relatively unaffected by the level of the applied gravity load, averaging 0.628 and 0.637 for the peripheral and the internal floor plates, respectively. This observation implies that a SDOF approximation can be used to describe the nonlinear static response of the considered floor plate upon impact. Based on this approximation, a linear compatibility condition can relate the deflection u_s in the middle of the grillage system to the deflection $u_{s,i}$ of any other component[5,6,13]:

$$u_{s,i} = \beta_i u_s \tag{17}$$

As noted before, the same approximation is assumed to be reasonably accurate for the dynamic response under impact loading, and hence the energy absorption of the floor is easily obtained as a weighted product of the static load resistance and a characteristic vertical displacement.

5.2.2. Modified Pseudo-Static Response

The next step following establishment of the nonlinear static response of the grillage floor

system is the shift of the axes of the static response P-u_s curve to account for the effect of the initial deformations of the lower floor plate under its original gravity loads. In this respect, the considered total floor gravity load P_o = 585kN results in a middle deflection of about 14mm regardless of the location of the floor plate. Based on the obtained shifted static response P′-u'_s curve, the full modified pseudo-static load-deflection response of the grillage system can be determined as explained in Section 3.

Since all the longitudinal secondary beams are assumed to sustain a UDL and deform in a triangular mode, the value of the weighting factors α_{SB1}, α_{SB2} and α_{SB3} can be taken as 0.5[5,6,13]. Moreover, the deformation compatibility factors (β_{SB1}, β_{SB2}, β_{SB3}) corresponding to the obtained grillage mode of deformation are equal to (0.628, 1.000, 0.628) and (0.637, 1.000, 0.637) for the peripheral and the internal floor plates, respectively. Therefore, work equivalence requires that the weighting factor α for the considered grillage floor system deforming according to the specific deformation mode should satisfy the following relationship:

$$\alpha\left(3P_{SB}\right)=\alpha_{SB1}\beta_{SB1}P_{SB}+\alpha_{SB2}\beta_{SB2}P_{SB}+\alpha_{SB3}\beta_{SB3}P_{SB} \tag{18}$$

which for the plate on the periphery of the building leads to:

$$\alpha=\frac{0.5\times1.000+2\times0.5\times0.628}{3}=0.376 \tag{19}$$

Similarly, the weighting factor α for the internal floor plate can be obtained from:

$$\alpha=\frac{0.5\times1.000+2\times0.5\times0.637}{3}=0.379 \tag{20}$$

As discussed in the presentation of the proposed assessment methodology, to establish the modified pseudo-static response of the grillage floor system, it is necessary to estimate the amount of energy transfer $E_{T,n,i}$ associated with the specific characteristics of the impact event under consideration. In the context of a thorough assessment strategy, several possibilities with respect to the amount of energy transfer that takes place during floor impact, covering the anticipated range between the two limiting cases of a fully plastic and a fully rigid impact, as well as various intensities of the gravity loads originally sustained by the falling floor are accounted for. Hence, the modified pseudo-static response of the considered grillage is

obtained herein for a range of non-dimensional energy reduction factors γ_i that specify the percentage of the initial kinetic energy of the impacting floor plate transferred to the impacted floor plate.

Figures 12a and 12b depict the modified pseudo-static load-deflection curves for the peripheral and the internal floor plates, respectively, corresponding to several γ_i factors from 20% to 70%. It is noted that the deflection is plotted up to the critical deformation level defined by shear failure at the outermost support joints of the intermediate longitudinal double-span secondary beam, while the right vertical axis indicates the percentage of the initial lower floor loads P_o that can be sustained as dynamic impact loading by the grillage system. Again, since the two considered floor plates fail in shear at a relatively early stage of the response, prior to the development of significant axial forces within the support joints of the transverse primary beam, their modified pseudo-static responses are practically identical. Based on Figs. 12a and 12b, it can be readily observed that the grillage floor system has limited modified pseudo-static capacity P' to arrest impact of the floor above. It is remarkable that even when a very low amount of energy transfer equal to 20% of the original kinetic energy of the falling plate is assumed, corresponding to a rather favourable plastic impact scenario, the impacted grillage system can only resist an impact loading that does not exceed 26% of its original gravity loads P_o. Also, for the almost certainly higher percentages of imparted energy associated with rigid impact possibilities, the modified pseudo-static capacity of the grillage system further decreases, with only an impact loading equal to 8% of P_o withstood when $\gamma_i = 70\%$.

To further highlight this observation, the following four impact scenarios involving the peripheral floor plate are investigated:

- Scenario 1 – plastic impact between the two floor plates is considered with the falling floor originally carrying half of the gravity loads of the lower floor. The occurring amount of energy transfer is estimated at 20% of the kinetic energy attained by the upper floor immediately before impact.
- Scenario 2 – same as Scenario 1 except that the two impacting floor plates initially carry equal gravity loads, and thus a higher percentage of the original kinetic energy of the falling floor equal to 30% is imparted to the lower floor.
- Scenario 3 – rigid impact between the two floor plates of Scenario 1 is taken into account, where 50% of the kinetic energy of the impacting floor is transmitted to the

impacted floor.

- Scenario 4 – the two floor plates of Scenario 2 are considered with rigid impact. Again, the proportion of energy transfer is estimated at 50% of the kinetic energy of the upper floor.

Table 9 summarizes the overall dynamic load carrying capacity P′ at the critical deformation level as well as the corresponding demand (expressed as a proportion λ of the initial lower floor loads P_o) for the four scenarios described above. It can be seen that the obtained Capacity/Demand ratios (or unity factors) are significantly lower than one in all cases. Moreover, the greatest discrepancy between the estimated modified pseudo-static capacity and the demand posed by the suddenly applied impact loading corresponds to Scenarios 2, 3, and 4, in which either the two floor plates are equally loaded or a rigid impact scenario is assumed. Hence, it can be easily concluded that in the event of failure and subsequent impact of a single floor plate onto the floor plate below, the lower impacted system, modelled using a grillage-type approximation, is highly unlikely to possess sufficient dynamic load carrying capacity to resist the imposed dynamic loads and prevent progressive collapse. This conclusion is further supported by the fact that all floors of the steel-framed composite building under consideration are originally designed to carry equal gravity loads.

The obvious vulnerability of the considered grillage floor system to impact from the floor above may to some extent be attributed to the premature shear failure mechanism that determines the floor limit state. With reference to the floor plate on the periphery of the building, a considerable improvement in the impact response can be achieved if the shear response is considered to be ductile, thus leading to a limit state defined by reinforcement rupture at the support joints of the intermediate secondary beam. In such case, the dynamic load carrying capacity P′ will increase substantially, varying from 124.44kN for γ_i = 70% to 373.94kN for γ_i = 20%, leading to improved unity factors as given in Table 10. Nevertheless, these results show that if the upper floor carries equal gravity load to the lower floor, the grillage system will still be unable to survive floor impact even in the best-case scenario.

Even though the presented assessment of the resistance of the floor plate to impact and subsequent progressive collapse draws a very negative picture, it is emphasised that this is based on a simplified grillage approximation of the actual floor plate response. An enhanced behaviour as well as a more realistic simulation of the floor response upon impact may be

achieved with a more detailed slab model of the nonlinear static response, capable of a more accurate representation of planar membrane action. Importantly, the outcome of the assessment relies greatly upon the effectiveness of the adopted mechanical joint models to accurately reproduce the behaviour of the partial-strength joints affected by this extreme event. It is therefore imperative that more research be carried out on various connection types, particularly involving experimental validation of their available ductility supply. This need is further highlighted by the identification of shear failure mechanisms, which may have a detrimental effect on the joint ductility supply. In this respect, an additional cause of concern is that a SDOF model based on a bending mode, similar to that considered in this study, can underestimate the shear forces under dynamic conditions, if these forces are determined from static equilibrium. Hence, even if the nonlinear static response does not exhibit shear failure, the shear forces may in fact be greater under the real dynamic loading. Since the proposed approach does not account for this effect, it should certainly be subject of future research.

6. Conclusions

This paper proposes a novel simplified framework for progressive collapse assessment of floor systems within multi-storey buildings, considering the impact of failed floors as an event-independent design scenario. The main advantage of the introduced methodology over other available approaches, which are either overly complicated/computationally demanding or unrefined/simplistic, is that it addresses the problem in a practical, yet theoretically sound manner, allowing for the relative significance of all the important robustness parameters, such as the energy absorption capacity, strength and ductility supply of the impacted floor, to be evaluated. The proposed assessment framework comprises three major independent stages, including: i) the establishment of the nonlinear static response of the impacted floor system using either simplified or detailed models, ii) a simplified dynamic assessment approach to estimate the maximum dynamic deformation demands upon impact, and iii) a ductility assessment, in which the overall ability of the impacted floor system to arrest impact and stop the progression of failure can be assessed based on the available ductility supply of its components. Hence, a new modified pseudo-static floor response is introduced, which forms the basis for a comprehensive assessment that collectively considers all the aforementioned structural robustness characteristics.

As the efficacy of the proposed method is directly related to the accurate estimation of the energy transfer that takes place during impact, a theoretical calculation has demonstrated that

the amount of energy imparted to a beam of the lower impacted floor in a fully plastic impact is approximately equal to 40% of the kinetic energy acquired by an identical falling beam immediately before impact. On the other hand, when a fully rigid impact is taken into account in association with a triangular deformation mode for the impacted floor beam, the resulting energy transfer can vary depending on the characteristics of the assumed rebound velocity profile, typically between 70% and 98% of the original kinetic energy of the impacting beam.

A series of numerical studies is also carried out with reference to the two limiting impact scenarios. It is concluded that the amount of energy imparted to the lower floor beam when plastic impact is assumed typically increases with increasing gravity loads sustained by the upper floor, and can vary from approximately 25% to 50% of the initial kinetic energy of the falling beam. Less energy transfer compared to the individual beams occurs when redundancy is considered, especially for heavily loaded falling floors, since the deformation mode of the impacted floor exhibits more localized deformations. Regarding rigid impact, the performed numerical studies have confirmed that the amount of energy transfer is generally higher than that associated with plastic impact, ranging between 50% and 70% of the kinetic energy acquired by the falling floor immediately before impact.

The application of the proposed progressive collapse assessment framework to a seven-storey steel-framed composite building with simple/partial-strength joints has clearly indicated that the impacted floor plate system, modelled as a grillage system, is highly unlikely to withstand impact of the floor above. Even for the least demanding impact scenario accounted for in this study, which involves a falling floor that only sustains half of the impacted floor gravity loads and assumes plastic impact with only 20% of the kinetic energy transferred, the estimated dynamic capacity of the impacted plate marginally exceeds 50% of the imposed demand. It is also notable that the development of shear failure mechanisms in association with the nonlinear static response of the grillage system cannot be deemed exclusively responsible for this distinct vulnerability since even a ductile mode of shear failure is unable to guarantee sufficient ductility supply that would prevent progressive collapse. Thus, although assessment is based on a simplified grillage-type approximation rather than a detailed slab model, the explicitness of the results leads to the conclusion that a floor system within a steel-framed composite building with a typical structural configuration has limited chances to arrest impact of an upper floor. This is particularly true when the falling floor completely disintegrates and falls as debris without retaining any residual strength or spanning capability.

In this context, the inability of the grillage system to arrest impact is to some degree related to the use of fin plate connection details for the beam-to-beam joints at the supports of the secondary beams. Hence, apart from the need for further static tests that will confidently establish the available ductility supply of this connection type, the extremely dynamic nature of the impact event also necessitates the performance of dynamic tests that can identify the real possibility of less well understood failure mechanisms, mainly related to shear and local buckling modes.

To conclude, although there is room for further improvements with respect to its accuracy and applicability, the proposed assessment methodology provides an effective platform to rationally tackle the scenario of floor impact, which is one of the most prevalent progressive collapse initiation mechanisms. The envisaged improvements mainly include the development of refined simplified floor models, experimental investigations of the joint ductility supply, as well as numerical and experimental studies on the effect of material rate sensitivity. Furthermore, additional numerical studies are needed to confidently estimate the amount of energy transfer with particular reference to the response of three-dimensional floor systems subject to rigid impact scenarios. Yet, even in its present form, the method is considered to err on the conservative side because it is based on the onerous assumption of the upper floor falling as debris. Therefore, given the complexity of the problem in hand, it can potentially constitute a useful design tool.

Acknowledgements

The authors would like to acknowledge the financial support provided for this work by ARUP and EPSRC under a Case award scheme. The significant input into this project of several ARUP staff, especially Faith Wainwright, Mike Banfi and Michael Willford, is also gratefully acknowledged.

7. References

1. General Services Administration (2003). "Progressive Collapse Analysis and Design Guidelines for New Federal Office Buildings and Major Modernization Projects," USA, June.

2. Office of the Deputy Prime Minister (ODPM) (2004). "The Building Regulations 2000, Part A, Schedule 1: A3, Disproportionate Collapse," London, UK.

3. American Society of Civil Engineers (ASCE) (2005). "Minimum Design Loads for Buildings and Other Structures," SEI/ASCE 7-05, Reston, VA, USA.

4. Department of Defense (DoD) (2005). "Unified Facilities Criteria, Design of Buildings to Resist Progressive Collapse," UFC 4-023-03, USA, January.

5. Izzuddin, B.A., Vlassis, A.G., Elghazouli, A.Y., and Nethercot, D.A. (2007). "Assessment of Progressive Collapse in Multi-Storey Buildings," *Buildings and Structures, Proceedings of the Institution of Civil Engineers*, **160**(SB4), pp. 197-205.

6. Izzuddin, B.A., Vlassis, A.G., Elghazouli, A.Y., and Nethercot, D.A. (2007). "Progressive Collapse of Multi-Storey Buildings due to Sudden Column Loss – Part I: Simplified Assessment Framework," *Engineering Structures*, **30**(5), pp. 1308-1318.

7. Vlassis, A.G., Izzuddin, B.A., Elghazouli, A.Y., and Nethercot, D.A. (2007). "Progressive Collapse of Multi-Storey Buildings due to Sudden Column Loss – Part II: Application," *Engineering Structures*, **30**(5), pp. 1424-1438.

8. Kaewkulchai, G., and Williamson, E.B. (2004). "Beam Element Formulation and Solution Procedure for Dynamic Progressive Collapse Analysis," *Computers and Strcutures*, **82**(7-8), pp. 639-651.

9. Kaewkulchai, G., and Williamson, E.B. (2006). "Modelling the Impact of Failed Members for Progressive Collapse Analysis of Frame Structures," *Journal of Performance of Constructed Facilities*, ASCE, **20**(4), pp. 375-383.

10. Watson, K.L. (1998). *Foundation Science for Engineers*, Second Edition, Macmillan Press Ltd, Basingstoke, Hampshire.

11. Jones, N. (1989). *Structural Impact*, Cambridge University Press, Cambridge.

12. Vlassis, A., Izzuddin, B., Elghazouli, A., and Nethercot, D. (2005). "Simplified Progressive Collapse Analysis of Floor Systems," *Proceedings of IABSE Symposium on Structures and Extreme Events*, Lisbon, Portugal, pp. 252-253 & CD.

13. Vlassis, A.G. (2007). *Progressive Collapse Assessment of Tall Buildings*, PhD Thesis, Department of Civil and Environmental Engineering, Imperial College London.

14. Izzuddin, B. A. (1991). *Nonlinear Dynamic Analysis of Framed Structures*, PhD Thesis, Department of Civil Engineering, Imperial College, University of London.

15. Faella, C., Piluso, V., and Rizzano, G. (2000). *Structural Steel Semirigid Connections: Theory, Design and Software*, CRC Press LLC, Boca Raton, FL.

16. Izzuddin, B.A. (1998). "Adaptive Contact Analysis of Framed Structures," *Proceedings of the 6th Association of Computational Mechanics in Engineering (ACME-UK) Annual Conference*, University of Exeter, Exeter, UK, pp. 147-150.

17. British Standards Institution (2001). "BS 5950-1:2000: Structural use of steelwork in building, Part 1: Code of practice for design – Rolled and welded sections," London, UK.

18. British Construction Steelwork Association/Steel Construction Institute (2002). "Joints in Steel Construction: Simple Connections," London, UK.

19. Jarrett, N. D. (1990). "Axial Tests on Beam/Column Connections," BRE Client Report CR 55/90, Building Research Establishment, Garston, Watford, UK.

20. Owens, G.W., and Moore, D.B. (1992). "The Robustness of Simple Connections," *The Structural Engineer*, **70**(3), pp. 37-46.

21. Jarrett, N. D., Grantham, R. I. (1993). "Robustness Tests on Fin Plate Connections," BRE Client Report GD 1101, Building Research Establishment, Garston, Watford, UK.

22. Anderson, D., Aribert, J. M., Bode, H., and Kronenburger, H. J. (2000). "Design rotation capacity of composite joints," *The Structural Engineer* 78(6), pp. 25-29.

Table 1 Energy transfer in a fully rigid impact (h = 4m, g =9.81m/s^2, v_1 = 8.86m/s)

v_{rs} (m/s)	v_m (m/s)	v_{rm} (m/s)	Initial energy	Final energy		Relative energy transfer E (%)
				Lower beam	Upper beam	
0.00	15.22	1.93	19.62 *mL*	19.31 *mL*	0.31 *mL*	98
4.00	14.87	-0.42	19.62 *mL*	18.41 *mL*	1.21 *mL*	94
5.00	14.66	-1.13	19.62 *mL*	17.90 *mL*	1.72 *mL*	91
6.00	14.39	-1.89	19.62 *mL*	17.27 *mL*	2.35 *mL*	88
7.00	14.07	-2.71	19.62 *mL*	16.51 *mL*	3.11 *mL*	84
9.00	13.22	-4.57	19.62 *mL*	14.56 *mL*	5.06 *mL*	74
12.97	9.89	-9.89	19.62 *mL*	8.15 *mL*	11.47 *mL*	41

Table 2 Maximum dynamic midspan deflection $u'_{d,max}$ due to plastic impact for simplified steel beam model (h = 4m)

m_1/m_2	$u'_{d,max}$ (mm)	
	L = 8m	L = 20m
0.5	215.5	341.1
1.0	592.9	820.8
2.0	1476.0	2219.4

Table 3 Energy transfer during plastic impact for simplified steel beam model (h = 4m)

L = 8m					
m_1/m_2	**W' (N mm)**	**U' (N mm)**	**E_T (N mm)**	**E_K (N mm)**	**E_T/E_K (%)**
0.5	8.27×10^6	88.05×10^6	79.78×10^6	312.81×10^6	25.5%
1.0	46.09×10^6	279.38×10^6	233.28×10^6	625.61×10^6	37.3%
2.0	230.14×10^6	831.79×10^6	601.66×10^6	1251.23×10^6	48.1%
L = 20m					
m_1/m_2	**W' (N mm)**	**U' (N mm)**	**E_T (N mm)**	**E_K (N mm)**	**E_T/E_K (%)**
0.5	4.95×10^6	37.55×10^6	32.61×10^6	125.12×10^6	26.1%
1.0	24.91×10^6	122.94×10^6	98.03×10^6	250.25×10^6	39.2%
2.0	137.28×10^6	394.40×10^6	257.13×10^6	500.49×10^6	51.4%

Table 4 Energy transfer during plastic impact for detailed composite beam model (h = 4m)

m_1/m_2	W' (N mm)	U' (N mm)	E_T (N mm)	E_K (N mm)	E_T/E_K (%)
0.5	5.65×10^6	89.07×10^6	83.42×10^6	325.20×10^6	25.7%
1.0	30.04×10^6	284.94×10^6	254.90×10^6	650.40×10^6	39.2%
2.0	153.58×10^6	804.31×10^6	650.73×10^6	1300.80×10^6	50.0%

Table 5 Energy transfer during plastic impact for grillage floor system (h = 4m)

m_1/m_2	W' (N mm)	U' (N mm)	E_T (N mm)	E_K (N mm)	E_T/E_K (%)
0.5	17.65×10^6	112.12×10^6	94.48×10^6	480.00×10^6	19.7%
1.0	62.25×10^6	279.07×10^6	216.82×10^6	960.00×10^6	22.6%
2.0	187.88×10^6	703.41×10^6	515.54×10^6	1920.00×10^6	26.9%

Table 6 Maximum dynamic midspan deflection $u'_{d,max}$ due to rigid impact for simplified steel beam model (h = 4m)

m_1/m_2	$u'_{d,max}$ (mm)	
	L = 8m	L = 20m
0.5	411.5	552.5
1.0	785.2	1011.6
2.0	1550.7	2438.0

Table 7 Energy transfer during rigid impact for simplified steel beam model (h = 4m)

L = 8m					
m_1/m_2	**W' (N mm)**	**U' (N mm)**	**E_T (N mm)**	**E_K (N mm)**	**E_T/E_K (%)**
0.5	15.93×10^6	184.14×10^6	168.21×10^6	312.81×10^6	53.8%
1.0	61.11×10^6	386.14×10^6	325.03×10^6	625.61×10^6	52.0%
2.0	242.02×10^6	888.09×10^6	646.07×10^6	1251.23×10^6	51.6%
L = 20m					
m_1/m_2	**W' (N mm)**	**U' (N mm)**	**E_T (N mm)**	**E_K (N mm)**	**E_T/E_K (%)**
0.5	8.26×10^6	74.63×10^6	66.37×10^6	125.12×10^6	53.0%
1.0	30.85×10^6	157.96×10^6	127.11×10^6	250.25×10^6	50.8%
2.0	150.91×10^6	439.77×10^6	288.85×10^6	500.49×10^6	57.7%

Table 8 Energy transfer during rigid impact for detailed composite beam model (h = 4m)

m_1/m_2	W' (N mm)	U' (N mm)	E_T (N mm)	E_K (N mm)	E_T/E_K (%)
0.5	3.87×10^6	119.87×10^6	116.00×10^6	162.60×10^6	71.3%
1.0	12.91×10^6	215.81×10^6	202.90×10^6	325.20×10^6	62.4%
2.0	53.38×10^6	482.02×10^6	428.64×10^6	650.40×10^6	65.9%

Table 9 Overall dynamic capacity and demand for the peripheral floor plate

Scenario No.	Capacity P′ (kN)	Demand λ P_o (kN)	Capacity/Demand ratio
1	150.6	292.5	0.51
2	104.0	585.0	0.18
3	64.2	292.5	0.22
4	64.2	585.0	0.11

Table 10 Unity factors corresponding to reinforcement rupture for the peripheral floor plate

γ_i (%)	Capacity P' (kN)	Demand λP_o (kN)	Unity factor
20	373.9	585.0	0.64
30	266.9	585.0	0.46
40	207.5	585.0	0.36
50	169.7	585.0	0.29
60	143.6	585.0	0.25
70	124.4	585.0	0.21

LIST OF FIGURES

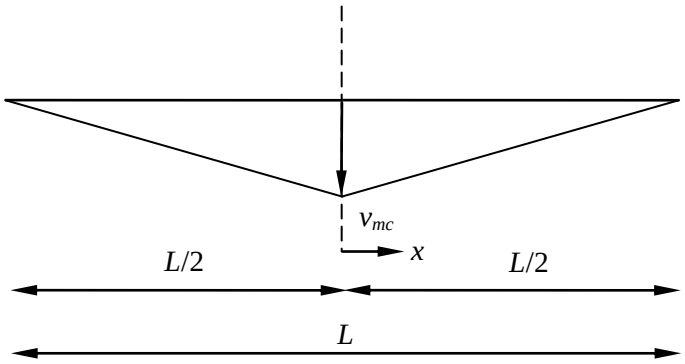

Figure 1 Velocity profile for the two combined beams after fully plastic impact.

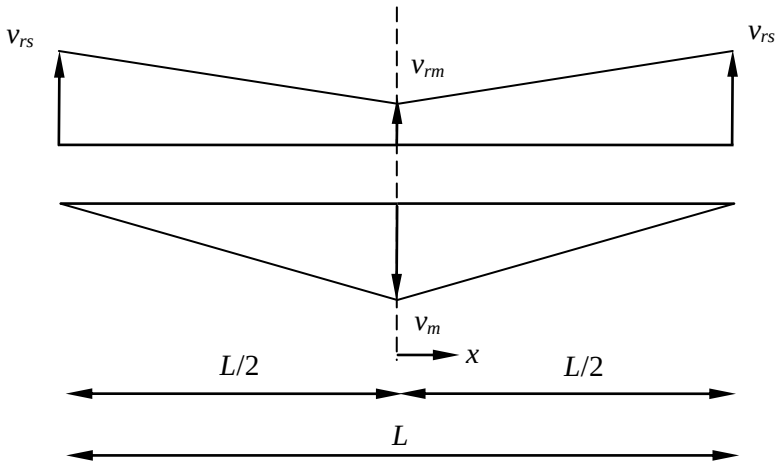

Figure 2 Velocity profile for the two independent beams after fully rigid impact.

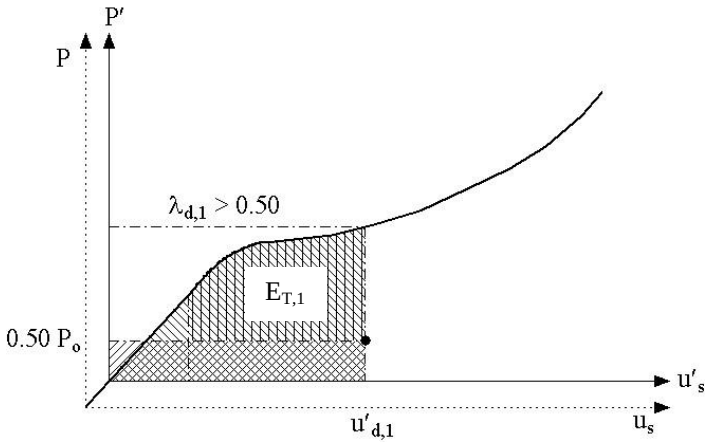

(a)

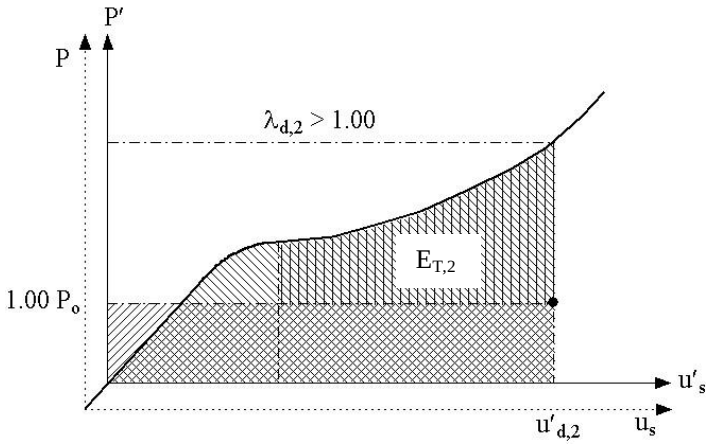

(b)

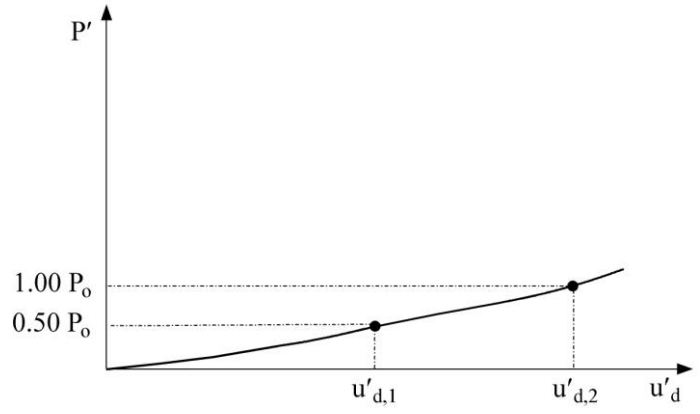

(c)

Figure 3 Simplified dynamic assessment and definition of modified pseudo-static response for impacted floor systems. (a) Dynamic response $P' = 0.50\ P_o$; (b) Dynamic response $P' = 1.00\ P_o$; (c) Modified pseudo-static response.

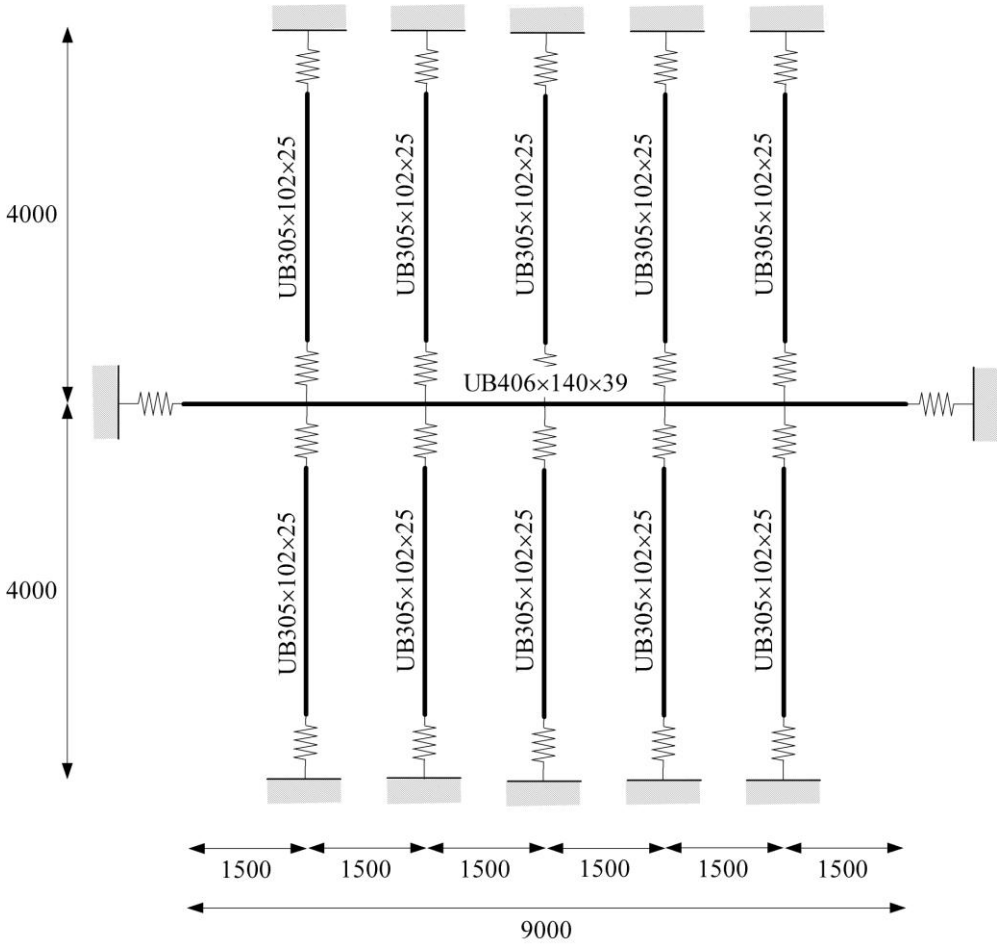

Figure 4 Plan view of grillage floor system (dimensions in mm).

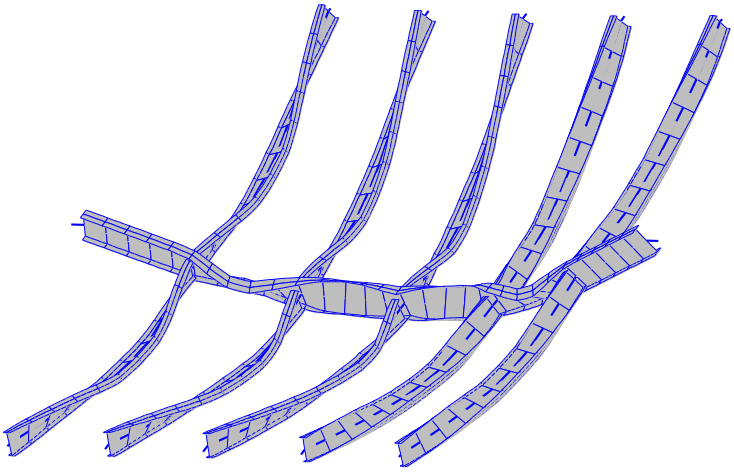

Figure 5 Deformed shape of grillage floor system for m_1/m_2 = 2.0 (h = 4m).

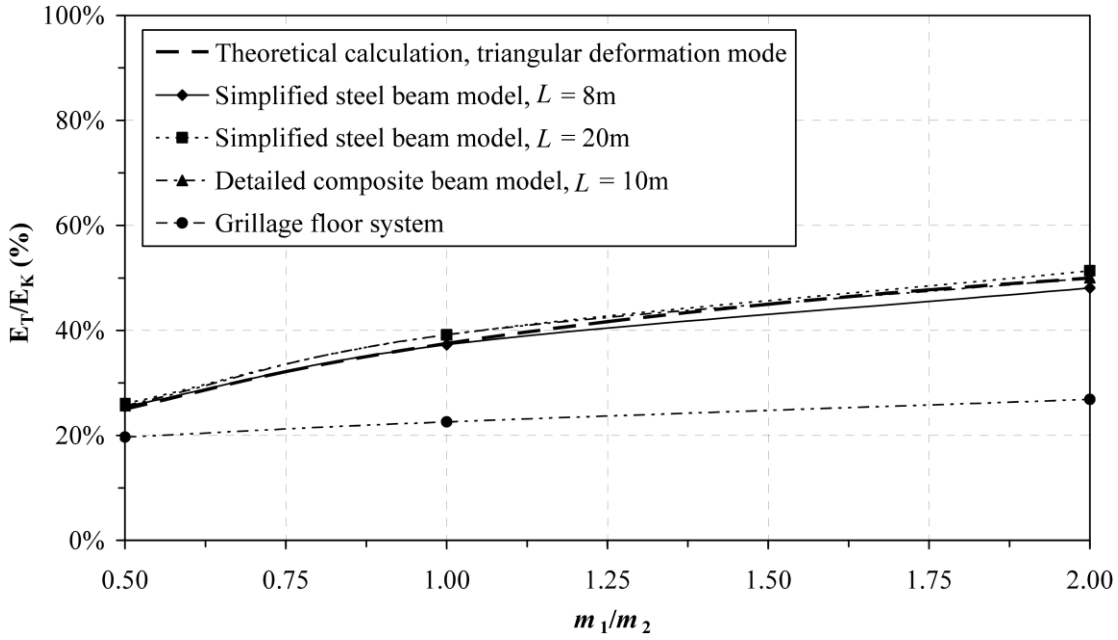

Figure 6 Variation of energy transfer with mass ratio of floors for plastic impact (h = 4m).

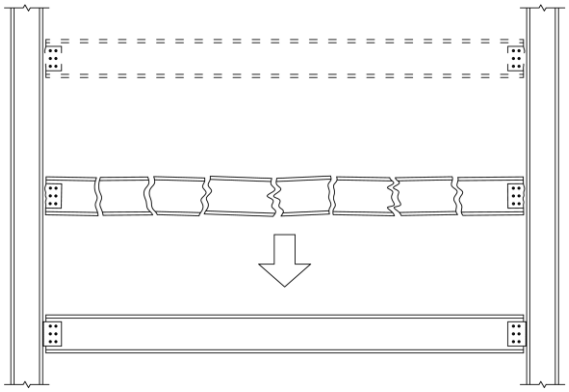

Figure 7 Failed floor falling as debris.

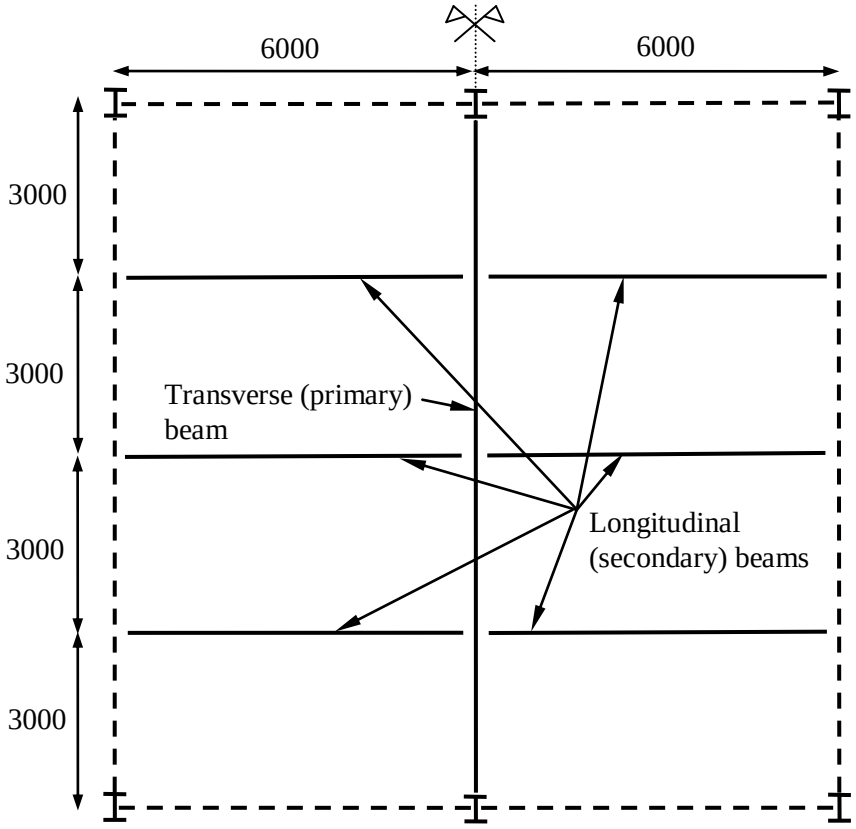

Figure 8 Plan view of the grillage system subject to upper floor impact (dimensions in mm).

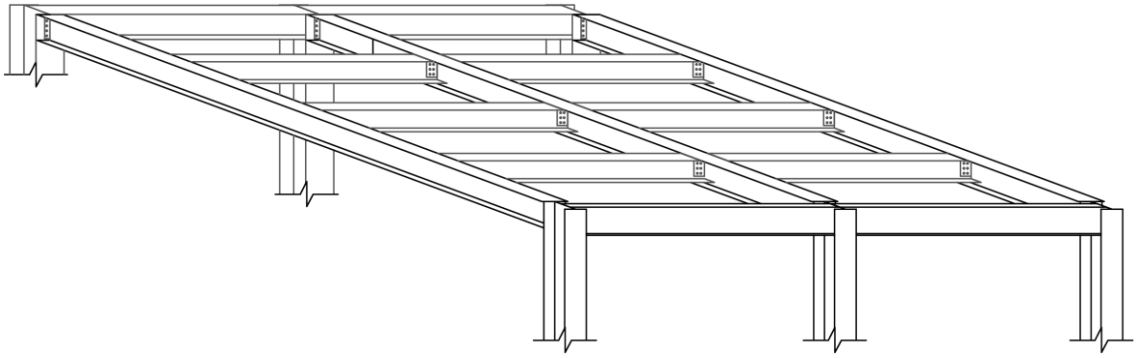

(a)

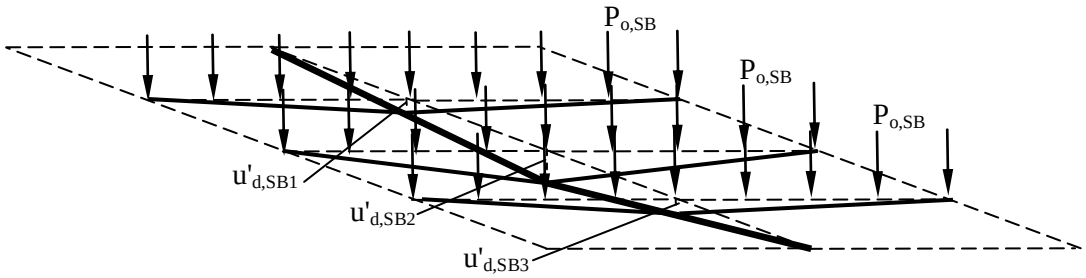

(b)

Figure 9 Floor impact assessment. (a) Original floor grillage; (b) Assumed initial gravity load distribution and approximate deformation mode upon impact.

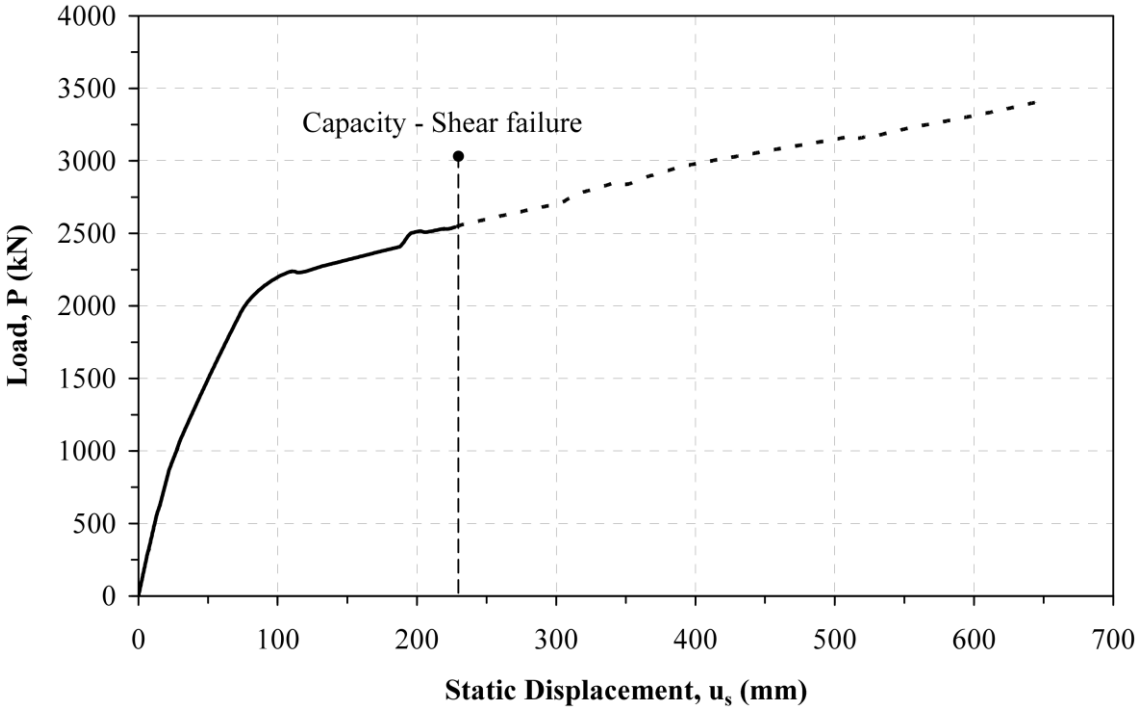

(a)

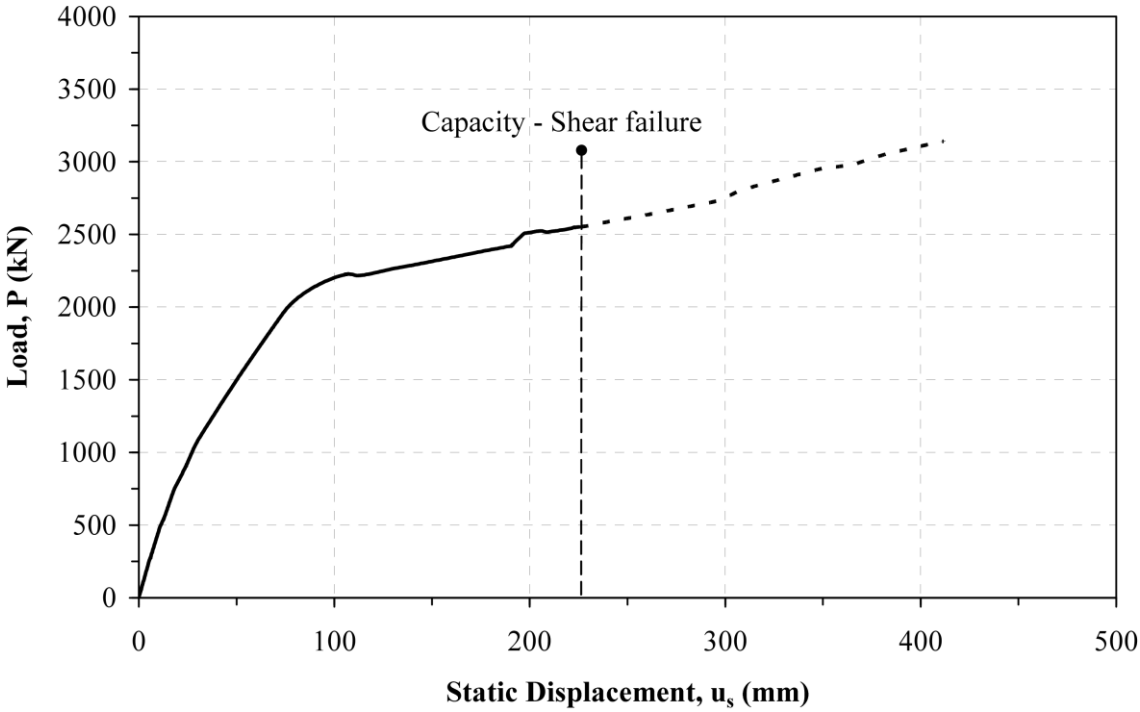

(b)

Figure 10 Static load-deflection curve for the grillage system. (a) Peripheral floor plate; (b) Internal floor plate.

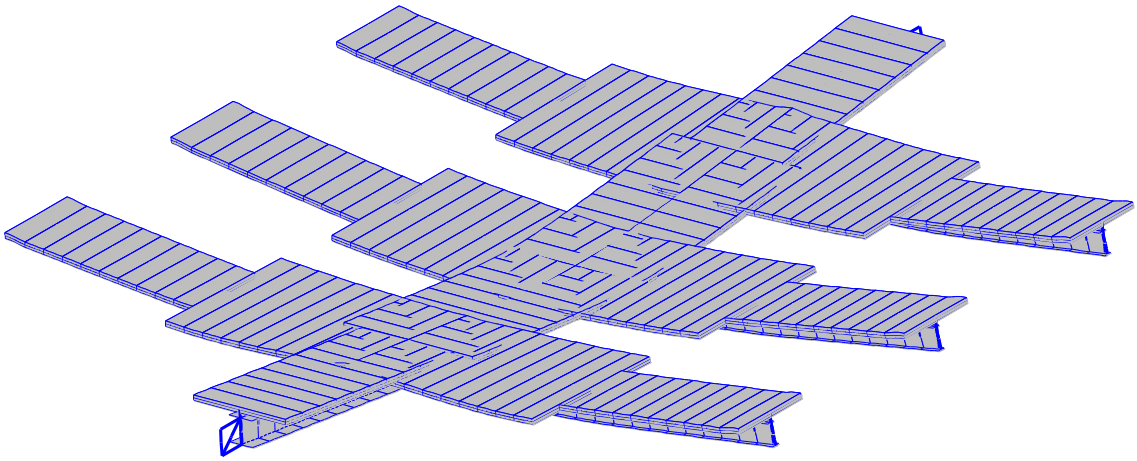

Figure 11 Deformed shape for the peripheral floor plate.

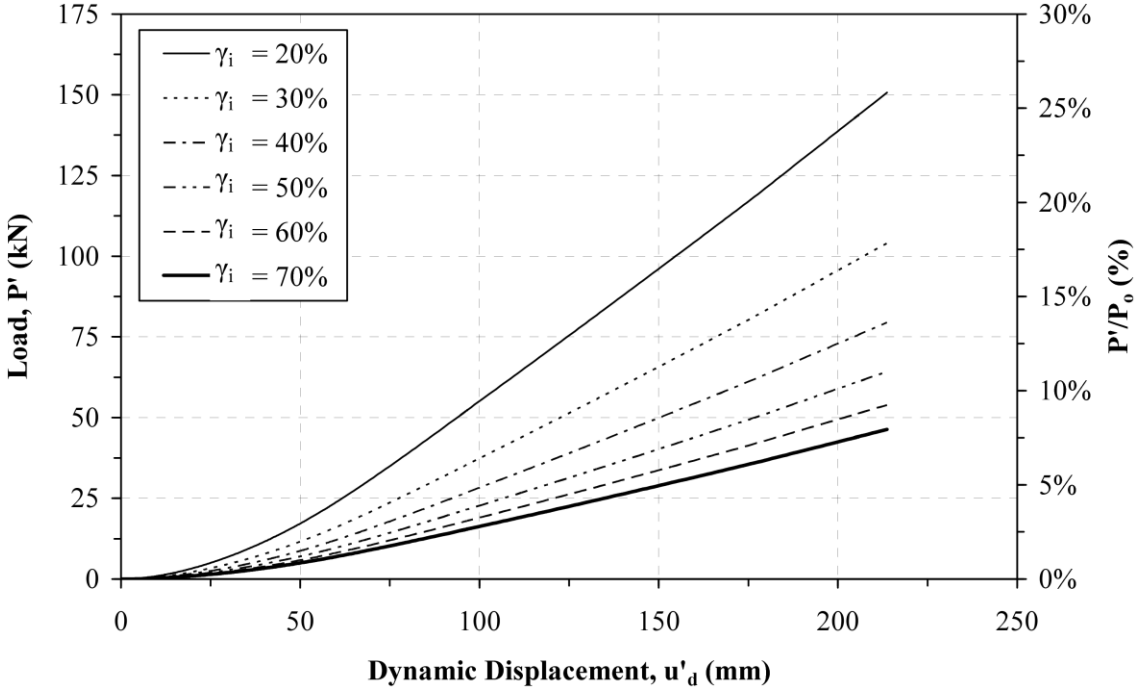

(a)

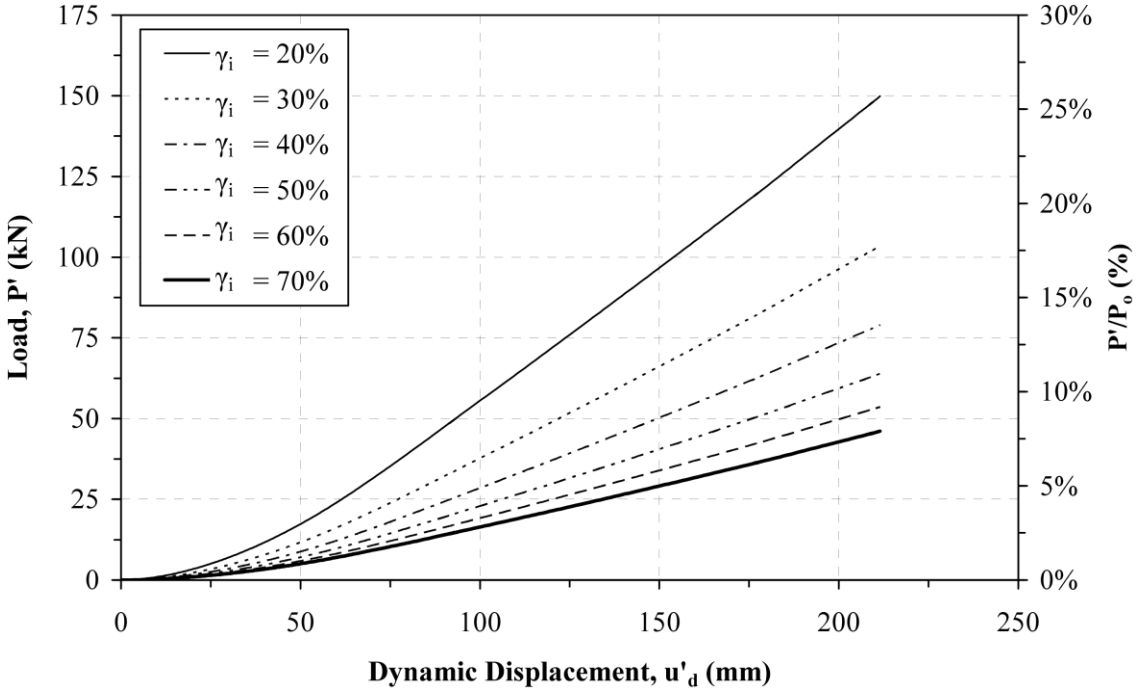

(b)

Figure 12 Modified pseudo-static load-deflection curves for the grillage system. (a) Peripheral floor plate; (b) Internal floor plate.